POSTBUCKLING BEHAVIOR OF GRAPHITE/EPOXY WING BOXES PANELS UNDER PURE TORSION

Giulio Romeo * Giacomo Frulla †
Politecnico di Torino - Dept. of Aerospace Eng.
C.so Duca degli Abruzzi 24, 10129 Turin, Italy

Abstract

This paper reports both the theoretical analysis and experimental results performed on advanced composite wing boxes under pure torsion. By taking into account the nonlinear effective shear modulus of skin panels operating during postbuckling, it is possible to obtain good correlation between the theoretical and the experimental behaviour. An incomplete diagonal shear stress field is used to calculate the effective shear modulus, that can be reduced by up to 50% in comparison to the unbuckled panels, thus causing a drastic reduction in the wing box's torsional stiffness. Furthermore, an analytical solution has been devoloped to investigate the postbuckling behaviour of anisotropic panels under pure shear and lateral pressure. By taking into account the large change in the area enclosed by the mid-line of the box wall, due to the rilevant out-of-plane skin panels deflection in the postbuckling range, it is possible to obtain a better correlation between the theoretical and the experimental behaviour. At a shear load triple that of buckling, our results revealed angles of twist up to 75% greater than those predicted by the linear analysis.

Nomenclature

A	area enclosed by midline of the box wall
A_{cF}, A_{cU}	effective skin area cooperating with flange, or cooperating with upright
$A_{es\alpha}$	average Young's modulus of skin laminate in α direction multiplied by thickness
A_F	cross sectional area of flange
A_U	cross sectional area of upright
A_{ij}	extensional stiffnesses
A_{66S}	shear extensional stiffness of skin laminate
A_{66W}	shear extensional stiffness of web laminate
a	distance between uprights
B,H,L	wing box width, height and length
C_{pq}	Unknown coefficients for deflection W
D_{ij}	flexural stiffnesses
E_1, E_2	lamina modulus in 1-2 directions
F	Nondimensional Airy function=$\psi/A_{22}h^2$
F_{hk}	Unknown coeff. for the Airy function
G_{12}, ν_{12}	lamina shear mod. and Poisson's ratio
k	diagonal-tension factor
M_t	torsion moment
N_F, N_U	load/width on flange and upright
N_{cF}, N_{cU}	load/width on effective skin area cooperating with flanges and uprights
N_{xy}	applied shear flow
N_{xycr}	buckling shear flow of panel
N_1, N_2	tensile and compressive load in wrinkles
t_F, t_U	flange and upright thickness
t_S, t_W	skin and web panel thickness
U	Strain Energy
u, v, w	Displacement components
W	Nondimensional out-of-plane deflection
α	angle of principal direction of buckle
θ	angle of twist of wing box
ξ, η, ζ	Nondimensional x,y,z coordinate
ψ	Airy function

Introduction

Composite aerospace structures are often designed so that they will not buckle below the limit load. Many of the analytical and experimental results available in the literature for composite panels under uniaxial compression or shear loading[1-3] report noticeable postbuckling behaviour before failure. These panels are usually tested separately from the main structure, which may yield erroneous results. Indeed, additional loads are created on wing-box panels when torsion loads are applied to the box beam. Torsion curvature, associated with shear load, causes a distributed load perpendicular to both upper and

*Associate Professor
†Aeronautical Eng, MSC

lower wing-box panels resulting in a lateral pressure. Additional effects are created by the structure when skin panels are in the postbuckling phase. A diagonal shear stress field[4] appears and the effective shear modulus diminishes as the stress increases. Consequently, the torsional stiffness of the whole wing box is no longer linear and considerably reduced[5]. Furthermore, a very large change in the area enclosed by the mid-line of the box wall, due to the rilevant out-of-plane skin panels deflection in the highest postbuckling range, is possible[6-8], thus causing a reduction in the wing box's torsional stiffness.

A nonlinear analysis is presented in this paper to investigate the postbuckling behaviour of anisotropic panels under combined biaxial compression, shear loads and lateral pressure; initial imperfections are also included in the analysis. The deflection of the orthotropic rectangular plate under combined lateral and inplane loads has been investigated by Chia[9]. The nonlinear terms have been included in this analysis and some theoretical results are reported for a simply-supported plate under uniaxial compression. However, analytical and experimental results of anisotropic panels under inplane shear and lateral pressure have not been found.

To be taken into account is, also, the highly nonlinear behaviour of specially orthotropic laminates under shear stress. The shear modulus G_{12} of these materials may vary by 50% at relatively low levels of shear stress[10]. Thus, the tangent modulus theory must be used to predict torsional behaviour. For angle-ply laminates such as those used in the present tests, the influence of the variation in G_{12} with shear stress was taken into consideration; this effect was not significant; only in the last test, carried out up to very high load, was noted a slight influence.

Theoretical Analysis

In a wing box under a pure torque (Fig. 1), the angle of twist θ is defined by Bredt's theory[4], and is extended to composite structures as

$$\theta = \frac{M_t L}{4A^2}\left(\frac{2B}{A_{66S}} + \frac{2H}{A_{66W}}\right) \qquad (1)$$

Theoretically, the shear extensional stiffness of laminates is constant up to N_{xycr}; however in practice, structures always exhibit an incomplete diago- nal shear stress field in panels operating in the postbuckling phase. As is well known[4], in this field the tension diagonal carries the majority of the shear stress, since the buckled diagonal cannot withstand any significant additional load. We therefore introduce k (characterizing the degree to which the diagonal tension is developed), defined by the empirical expression[4]

$$k = \tanh[0.5\log(N_{xy}/N_{xycr})] \qquad (2)$$

this allows N_{xy} to be divided (Fig. 2) into a pure shear component N_{xyPS} and a diagonal tension component N_{xyDT} by

$$N_{xy} = N_{xyPS} + N_{xyDT} \qquad (3)$$

$$N_{xyDT} = kN_{xy} \qquad N_{xyPS} = (1-k)N_{xy} \qquad (4)$$

A value of $k = 0$ signifies an unbuckled panel; in this case, the panel is subjected to tension and compression loads, per unit width, of the same value as the applied shear flow along two diagonals oriented at $\pm 45°$ with respect to the sides. A value of $k = 1$ signifies a panel in pure diagonal tension (DT); here the panel is subjected to a tension load $N_1 = 2N_{xy}/\sin(2\alpha)$ along one diagonal oriented at an angle α, while along the second diagonal no compression load, per unit width, is applied. In the incomplete diagonal tension (IDT), the superposition of the two load systems gives the true load system.

Determination of the Angle α

Let us consider a panel delimited by two flanges and two uprights under shear flow (Fig. 3); it has been assumed in Ref. 4, that in a controlled diagonal tension field the isotropic skin panel may also carry compressive stresses parallel to the flanges or to the uprights. The loads per unit width in flanges, uprights (or ribs), and in the effective width of the anisotropic panel cooperating with them, have been determined in Ref.5. The α angle value of interest here is that which minimizes the total strain energy of the system U_{tot} with respect to α:

$$\frac{\partial U_{tot}}{\partial \alpha} = \frac{\partial U}{\partial \alpha} + \frac{\partial U_F}{\partial \alpha} + \frac{\partial U_U}{\partial \alpha} = 0 \qquad (5)$$

in which U is the strain energy of the panel in a diagonal tension field neglecting loads deriving from the pure shear field, U_F is the strain energy of the flanges and cooperating part of the panel, U_U is the strain energy of the uprights and cooperating part of the panel. The following expression of the strain energy will be used in the subsequent calculations

$$U = \frac{1}{2}\int_V \sigma\epsilon dV = \frac{1}{2}[N_1^2 ab/(A_{es\alpha})] \qquad (6)$$

in which

$$N_1 = \frac{kN_{xy}}{\sin(\alpha)\cos(\alpha)} \tag{7}$$

Finally, the angle α is obtained by assigning a stationary value to the total strain energy of the plate with respect to α, leading to:

$$\tan^2\alpha = \frac{\frac{kN_{xy}}{A_{es\alpha}}\frac{\sin^2\alpha-\cos^2\alpha}{\sin\alpha\cos^3\alpha}+\frac{N_FA_F}{g_Ft_F}+\frac{N_{cF}A_{cF}}{g_Ft_S}}{(\frac{N_UA_U}{q_Ut_U}+\frac{N_{cU}A_{cU}}{q_Ut_S})} \tag{8}$$

since α is enclosed in both terms of Eq. (8), an iterative cycle is necessary in order to obtain the final value, which usually lies between $45-37$ deg. As the angle of diagonal tension is known, it is possible to determine the extensional shear stiffness of laminate in this field, as shown below.

Determination of the Plate Equivalent Stiffness

The expression of the effective shear extensional stiffness of the diagonal tension anisotropic panel has been obtained by applying the principle of virtual work[5].

$$\frac{1}{A_{66DT}} = \frac{1}{A_{es\alpha}\sin^2\alpha\cos^2\alpha}+\frac{b\cot^2\alpha}{g_F}+\frac{a\tan^2\alpha}{q_U} \tag{9}$$

In the incomplete diagonal tension field, the superposition of the two shear strain deformations [Eq. (3)] gives the true shear extensional stiffness of the panel

$$\frac{1}{A_{66IDT}} = \frac{1-k}{A_{66PS}}+\frac{k}{A_{66DT}} \tag{10}$$

it is then possible to determine the effective angle of twist θ of the wing box [Eq. (1)] for different values of the applied shear stress. By applying Eqs. (8) and (9) to the isotropic panel, the same expressions reported in Ref. [4] are obtained.

A calculation illustrating the use of this theoretical model is reported in Appendix A of Ref. 5 for one of the wing boxes tested.

Determination of the Area enclosed by the box wall

With respect to the unbuckled wing box skin panel, the out-of-plane deflection of the skin has to be determined for taking into account the very large deflection at which the panel is subjected when operates in the highest postbuckling range.

The classical laminate theory has to be modified for the large deflection and postbuckling analysis of anisotropic plates under combined biaxial compression, shear loads and lateral pressure. The strain-displacement relations become nonlinear when the components due to the out-of-plane deflection are taken into account. Plates with the initial imperfections w_0 have been studied on the basis of the Marguerre approximate nonlinear theory[6-9]. The resultant strain-displacement relations are

$$\epsilon_x = u_{,x}+\tfrac{1}{2}w_{,x}^2+w_{0,x}w_{,x}-zw_{,xx}$$

$$\epsilon_y = v_{,y}+\tfrac{1}{2}w_{,y}^2+w_{0,y}w_{,y}-zw_{,yy}$$

$$\epsilon_{xy} = u_{,y}+v_{,x}+w_{,x}w_{,y}+w_{0,y}w_{,x}+w_{0,x}w_{,y}-2zw_{,xy} \tag{11}$$

By using the principle of the stationary value of the total potential energy, the equilibrium equations are worked out. The compatibility equation, for panels with initial imperfections, is further used. By introducing the Airy function $\psi(x,y)$ as

$$N_x = \psi_{,yy} \quad , \quad N_y = \psi_{,xx} \quad , \quad N_{xy} = -\psi_{,xy} \tag{12}$$

and by substituting the stress-strain relations, in terms of the ψ function and the out-of-plane displacement, the following nondimensional governing system is obtained for symmetric panel:

$$\overline{D}_{11}^*W_{,\xi\xi\xi\xi}+4\overline{D}_{16}^*\lambda W_{,\xi\xi\xi\eta}+2(\overline{D}_{12}^*+2\overline{D}_{66}^*)\lambda^2W_{,\xi\xi\eta\eta}$$
$$+4\overline{D}_{26}^*\lambda^3W_{,\xi\eta\eta\eta}+\overline{D}_{22}^*\lambda^4W_{,\eta\eta\eta\eta}-\lambda^2(F_{,\eta\eta}W_{,\xi\xi}$$
$$+F_{,\xi\xi}W_{,\eta\eta}-2F_{,\xi\eta}W_{,\xi\eta}+F_{,\eta\eta}W_{0,\xi\xi}$$
$$+F_{,\xi\xi}W_{0,\eta\eta}-2F_{,\xi\eta}W_{0,\xi\eta})-\overline{q}=0 \tag{13}$$

$$\overline{A}_{11}^*\lambda^4F_{,\eta\eta\eta\eta}-2\overline{A}_{16}^*\lambda^3F_{,\xi\eta\eta\eta}+(2\overline{A}_{12}^*+\overline{A}_{66}^*)\lambda^2F_{,\xi\xi\eta\eta}$$
$$-2\overline{A}_{26}^*\lambda F_{,\xi\xi\xi\eta}+\overline{A}_{22}^*F_{,\xi\xi\xi\xi}=\lambda^2(W_{,\xi\eta}^2-W_{,\xi\xi}W_{,\eta\eta}$$
$$+2W_{0,\xi\eta}W_{,\xi\eta}-W_{0,\eta\eta}W_{,\xi\xi}-W_{0,\xi\xi}W_{,\eta\eta}) \tag{14}$$

The usual four types of boundary conditions along the edges of the panel are studied[7-8]; several conditions have to be satisfied for each boundary.

By defining the nondimensional applied inplane loads η_ξ^*,η_η^*, $\eta_{\xi\eta}^*$ as:

$$\eta_\xi^* = \frac{N_xb^2}{h^2A_{22}} \quad \eta_\eta^* = \frac{N_yb^2}{h^2A_{22}} \quad \eta_{\xi\eta}^* = \frac{N_{xy}b^2}{h^2A_{22}} \tag{15}$$

To satisfy the boundary conditions the assumed

functions are chosen in the following form

$$F = \eta_\xi^* \eta^2/2 + \eta_\eta^* \lambda^2 \xi^2/2 - \lambda \eta_{\xi\eta}^* \xi\eta + \sum_{h=1}^{m}\sum_{k=1}^{n} F_{hk} X_h Y_k \tag{16}$$

$$W = \sum_{p=1}^{i}\sum_{q=1}^{j} C_{pq}\omega(\xi,\eta) \tag{17}$$

$$W_0(\xi,\eta) = T\sin(\pi\xi)\sin(\pi\eta) \tag{18}$$

where X and Y are the characteristic clamped-clamped beam functions[8]. While the Airy function remains the same, the function $\omega(\xi,\eta)$ is chosen according to the boundary conditions to be:

a) BC-1 $\omega(\xi,\eta) = \sin(h\pi\xi)\sin(k\pi\eta)$
b) BC-2 $\omega(\xi,\eta) = X_h(\xi)\sin(k\pi\eta)$
c) BC-3 $\omega(\xi,\eta) = X_h(\xi)Y_k(\eta)$
d) BC-4 $\omega(\xi,\eta) = \sin(h\pi\xi)Y_k(\eta)$

The nondimensionalized transverse load $\overline{q}$ has been expanded in double trigonometric series as

$$\overline{q} = \sum_m \sum_n q_{mn}\sin(m\pi\xi)\sin(n\pi\eta) \tag{19}$$

If the load $\overline{q}$ is uniform, then

$$q_{mn} = \begin{cases} 16\overline{q}^o/\pi^2 mn & for\ odd\ m,n \\ 0 & for\ even\ m,n \end{cases} \tag{20}$$

Lateral pressure. As the result of the torsion curvature, the shear load applied in the upper and lower wing box panels are not aligned with respect to each other; vector addition therefore results in a lateral load. On the assumption that the Engineer's Theory of Bending (ETB) holds, the lateral pressure q^o applied to each of the wing box anisotropic panels is finally calculated as

$$q^o = M_t\theta/Aa \tag{21}$$

Solution Method. A set of nonlinear algebraic equations (the governing system) in terms of F_{hk} and C_{pq} and in terms of calculated Galerkin coefficients has been obtained by using the Galerkin procedure in Eq. (13) and Eq. (14).

The POBUCK computer program[6-8] has been developed to solve the set of nonlinear algebraic, resultant from Eq. (13) and (14), using an iterative procedure in order to find the postbuckling path at a certain load level. After possible values have been assigned to the unknowns C_{pq}, the first step consists of extracting F_{hk} from the second equation and substituting it into the first one. The next step is to solve this final nonlinear system as a function of the C_{pq} unknowns and thereby work out the C_{pq}. The scientific library software available from ABACI[12] is then employed to solve the final nonlinear system, using as a base the modified Powell hybrid method for finding the zero of a system of nonlinear functions. The user provides a subroutine which calculates the functions and the ABACI code calculates the jacobian by a forward-difference approximation. The iteration is developed until convergence with C_{pq} is reached, within 0.5% . The new minimum total potential energy configuration (also with different numbers of half-waves) is obtained, starting with the last solution of C_{pq} for subsequent load levels. If convergence has not been reached in this way, one can assign different initial C_{pq} values. The ABACI software used for solving the nonlinear system quickly converges to a solution without noticeable problems. As the out-of-plane deflection of the wing box panel is calculated, is then possible to obtain the variation of the area enclosed by midline of the box wall and, finally, the corrected value of angle of twist.

The POBUCK software operates on an IBM PS2 or higher, requiring about five minutes of CPU time with 36 terms, using NDP Fortran.

Experimental Tests

Starting from the above considerations, pure torsion tests were carried out on two wing box beams with a rectangular cross section; two graphite/epoxy prepreg materials (M40/914 VICOTEX and T300/F263 HEXCEL) were used for manufacturing the specimens.

The boxes consist of four corner flanges and four panels; four L aluminium flanges (30x30mm, 3 or 5 mm thick) were used at the corners. After the autoclave curing, the skin and web panels were bolted to the flanges along their entire length (see Table 1 for their geometrical properties). Both the full dimensions as well as the dimensions of box wall midline or bolt line are reported. The lay-up of the web panel is twice that of the skin. Both specimens were initially tested without a rib bolted at the centre of the wing box, and on a second occasion were tested with such a rib. Two thin flat aluminium plates (possessing a very high inplane stiffness and very low out-of-plane stiffness) were bolted to the ends of the boxes in order to attach them to the torsion machine (Fig.4)[11]. This is composed of a basement (A) where at its four corners there are two fixed columns (B), one connecting rod (C) and a hydraulic jack (I). The jack is used to apply the external load, which is then converted

into a twist moment by two thick, stiff flat plates (E), to which the box's thin aluminium plates are bolted (L). The thick plates (E) are connected to the frame by ball bearings (F) and floating rods (G), allowing the box to be regarded as a free warping twist problem without the introduction of corrective stresses.

TABLE 1 - Panel and cross-section dimensions of wing box n.2 and n.3 tested under pure torsion[a].

	wing box n.2	wing box n.3
lay-up	$(45_2/-45_2/0_3/90)_s$	$(-45_2/45_2/0_3/90)_s$
L	790(768)	790(768)
a	384	384
B	404(400)	404(400)
H	135(133)	135(133)
t_s	2	2.35
t_W	4	4.62
t_F	3	5
t_U	2	2

[a] All dimensions are in millimeters

The twist moment was applied step by step; deflection data for the lower box panel were taken at different load levels by means of an electrical transducer mounted on a computer-controlled slideway. Strains were measured by several linear and rosette strain gauges placed back-to-back on both the upper and lower panels at half, a quarter and three quarters of the length.

Material properties used in the analysis were experimentally determined to be:

M40/914: $E_1 = 209.6$ GPa; $E_2 = 6.89$ GPa;
$G_{12} = 4.26$ GPa; $\nu_{12} = 0.305$.

T300/F263: $E_1 = 132.63$ GPa; $E_2 = 9.2$ GPa;
$G_{12} = 4.54$ GPa; $\nu_{12} = 0.339$.

The theoretical buckling load of the skin panel subjected to shear load was determined by the computer code POBUCK. A summary of the results obtained for the four tests is reported in Table 2. A very good correlation between analytical buckling loads and experimental results was obtained.

Experimental Results

The angle of twist between the bulkheads as a function of the applied torsion moment is reported in Fig. 5 for the four wing box beams. The linear behaviour traced here was determined by Eq. (1), in which the shear extensional stiffnesses are considered constant; it clearly varies considerably from the experimental results. However, the influence of the variation of A_{66S} is evident, since the panel operated in an incomplete diagonal tension field. In this situation, the shear stiffness [Eq.(10)], changes as a function of the shear flow, modifying considerably the torsional stiffness of the wing box. The variation of the lamina shear modulus G_{12} was enclosed in calculating the skin shear stiffness; its value changed from 4.54 MPa up to 1.89 MPa at a torsion moment of 17.1 kNm; however, the effect of this variation on the angle of twist was of only 5.8%.

TABLE 2 - Shear buckling analytical results of the skin panel of the two wing boxes.

	wing box n.2		wing box n.3	
	one bay	two bay	one bay	two bay
N_{xycr} (N/mm)	21.01	34.19	35.72	56.59
M_{Tcr} (kNm)	2.27	3.69	3.77	5.97

A very high torsion moment was applied to the wing box n.3 with the bolted rib; up to a torsion moment of 10-11 kNm, the only influence affecting the nonlinear behaviour of the wing box was that of the skin shear stiffness operating in the IDT field. However, as consequence of the out-of-plane deflection of the skin panel operating in the postbuckling range, the variation of the area enclosed by the box wall midline was not negligible (10% at a torsion moment of 17.1 kNm); this effect, as well as the lateral pressure (maximum value of 0.0385 MPa), has also been introduced by the present theory, as reported in the theoretical analysis, and plotted in Fig. 5d. A very good correlation was obtained between the results determined by the present theoretical analysis and the experimental ones.

The experimental strain and deflection curves obtained from the test of wing box n.3 with the bolted rib are reported in Figs 6 and 7. Figure 6 shows experimental strains as a function of the applied torsion moment, measured by two back-to-back rosettes placed at one quarter length of the lower skin panels (L/4, B/2). The reported mean value of the two rosettes is considered to be the membrane value. Shear strain (Fig.6a) was almost constant along the thickness, and quite linear with the moment, up to a value of 6.3 kNm. From this point, however, we can clearly see the nonlinear behaviour of membrane shear strain due to buckling. Linear strains measured by back-to-back gauges bonded on the panel at 45 degrees, diagonal in compression, are reported in Fig.

6b; buckling is also evident and clearly demonstrated by a strain reversal.

With reference to Fig.2, it is possible to obtain, in the IDT field, minumum and maximum strains along the two principal directions oriented at an angle α and $\alpha+90$ degrees; they are reported in Fig. 6c and 6d and compared with the experimental strains measured by the back-to-back rosettes, although they are bonded on the crest of the wave. While a very good correlation was obtained for the compressive strain, a slight difference was noted for the tensile strain, at the highest applied loads.

Since in the IDT field, flanges and uprights apply to the skin panel a tensile load, back-to-back strain gauges were bonded to the skin near to the flanges. The measured strains in the upright direction are reported in Fig. 6e, and the membrane values compared with the analytical one, shown also in this case a good correlation.

Figure 7 shows the experimental deflections measured in 48 points of the lower panel, at two values of applied twist moment; one can easily detect the influence of the buckling waves on the panel's deflection. Results very similar to those shown were obtained for the other three tests at different applied twist moment.

In the two wing boxes with the bolted rib, testing was performed up to the failure torsion moments of 12.2 kNm and 18.2 kNm respectively. Failure resulted in a delamination of the skin panels as a consequence of the very high deflection wave of the buckled panel. Of note is the fact that the failure load was approximately one-third that predicted by classical lamination theory applied to an unbuckled panel under inplane shear.

Conclusion

A good correlation between theoretical analysis and experimental results was obtained for wing boxes under pure torsion by considering the effects of the nonlinear shear modulus of panels operating under an incomplete diagonal shear stress as well as the large change in the area enclosed by the mid-line of the box wall, due to the rilevant out-of-plane skin panels deflection in the postbuckling range. Although it was confirmed that composite panels can operate in the postbuckling field, these tests clearly demonstrate that the buckling of panels can drastically reduce the effective torsional stiffness of the structure as a whole. Consequently, static and dynamic behaviour of an entire wing may be changed, modifying the performance of aircraft.

References

[1]Starnes,J.H., Dickson,J.N., and Rouse,M., "Postbuckling Behaviour of Graphite-Epoxy Panels", *Proceedings of ACEE Composite Structures Technology*, 1984, pp. 137-159 (NASA CP 2321).

[2]Rouse,M., "Postbuckling of Flat Unstiffened Graphite-Epoxy Plates Loaded in Shear", *Proceedings of the AIAA/ASME/ASCE/AHS 26th S.S.D.M. Conf.* (Orlando, FL), AIAA, Washington, DC, 1985, pp. 605-616 (AIAA CP 851).

[3]Romeo,G., and Gaetani,G., "Effect of Low Velocity Impact Damage on the Postbuckling Behaviour of Composite Panels", *Proceedings of the 17th ICAS Congress* (Stockholm, Sweden), Vol. I, AIAA, Washington, DC, 1990, pp. 994-1004.

[4]Kuhn,P., *"Stresses in Aircraft and Shell Structures"*, 1st ed., McGraw-Hill, New York, 1956.

[5]Romeo,G., Frulla,G., Busto,M.: "Nonlinear Angle of Twist of Advanced Composite Wing Boxes under Pure Torsion". *AIAA Journal of Aircraft*, Vol.31, No.6, Nov-Dic. 1994, pp. 1297-1302.

[6]Romeo,G., and Frulla,G.: "Nonlinear Analysis of Graphite/Epoxy Wing Boxes under Pure Bending Including Lateral Pressure". *AIAA Journal of Aircraft*, Vol.32, N.6, Nov-Dec. 1995, pp. 1375-1381.

[7]Romeo,G., and Frulla,G.: "Nonlinear Analysis of Anisotropic Plates with Initial Imperfections and Various Boundary Conditions Subjected to Combined Biaxial Compression and Shear Loads". *Int. Journal of Solids and Structures*, Vol.31, No.6, pp.763-783, 1994.

[8]Romeo,G., and Frulla,G., "Postbuckling Behaviour of Anisotropic Plates under Biaxial Compression and Shear Loads", *Proceedings of the 18th ICAS Congress* (Beijing, P.R. China), Vol. II, AIAA, Washington, DC, 1992, pp. 1936-1944.

[9]Chia,C.Y. *Nonlinear Analysis of Plates*, McGraw-Hill, New York, 1980.

[10]Garber,D.P., "Tensile Stress-Strain Behaviour of Graphite/Epoxy Laminates", NASA CR-3592, Aug. 1982.

[11]Antona,E., and Gabrielli,G., "Un'Indagine Sperimentale su Strutture Alari a Cassone Soggette a Torsione (Experimental Investigation of Wing Box Structures under Pure Torsion)", *l'Aerotecnica Missili e Spazio*, No.1, Feb. 1974, pp. 13-24 (in Italian).

[12]Abaci,C., *The Scientific Desk - User Guide*, Raleigh, NC, 1987.

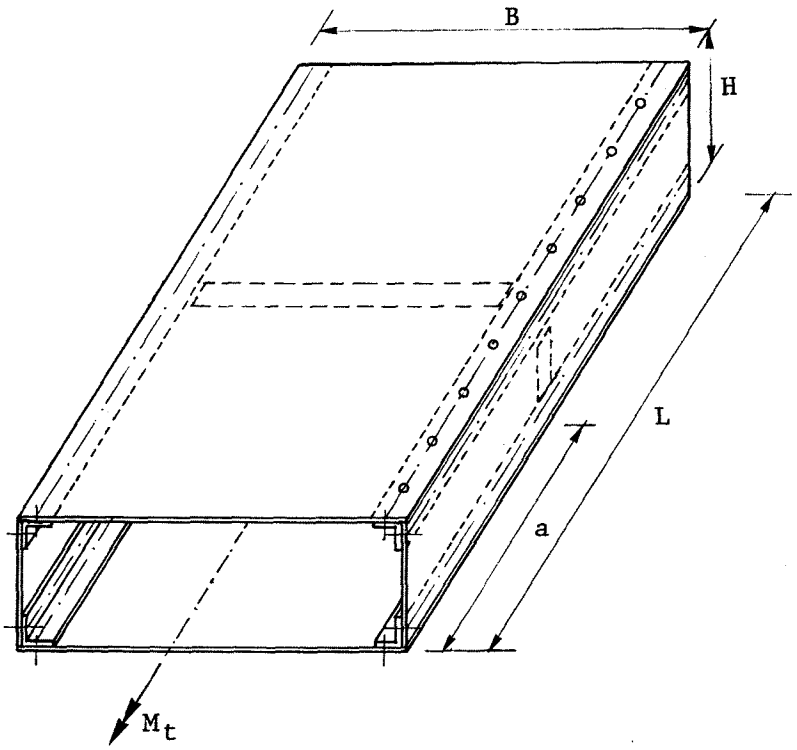

FIGURE 1 - Wing box structure under torsion

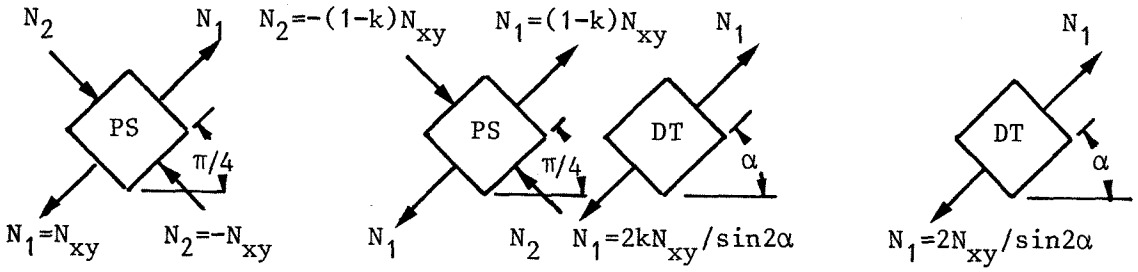

FIGURE 2 - State of loads in the skin panel for an Incomplete Diagonal Tension field.

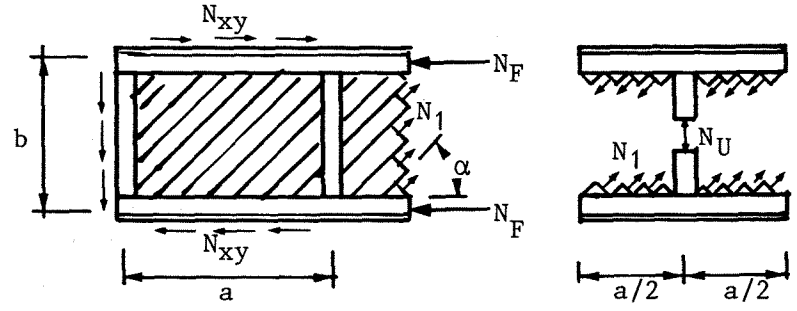

FIGURE 3 - State of loads for a IDT field.

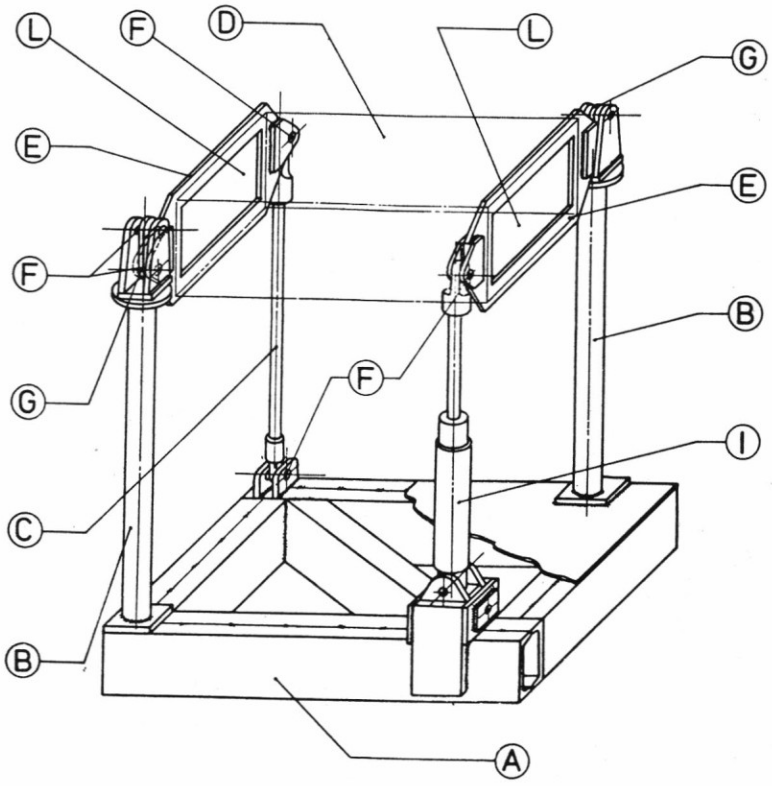

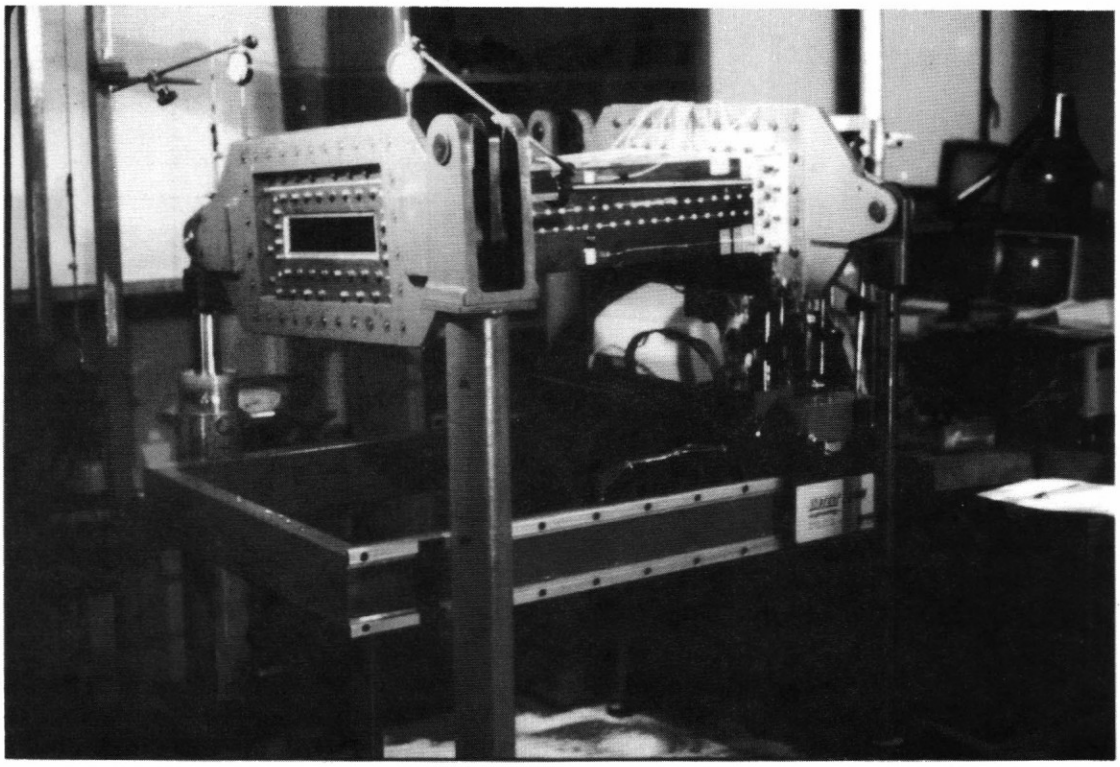

FIGURE 4 - Overall view of the torsion machine.

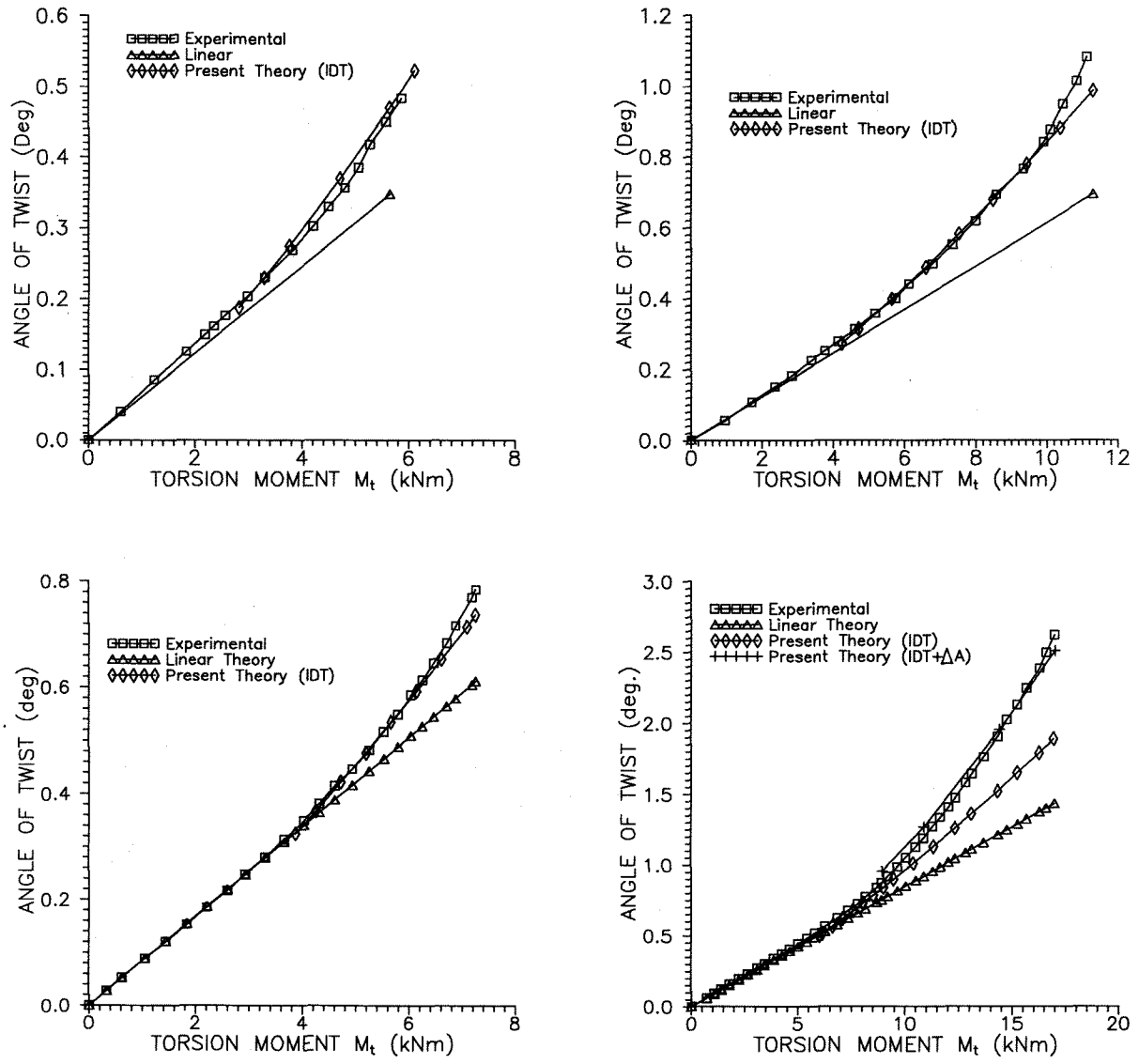

FIGURE 5 - Experimental and analytical angle of twist θ versus M_t considering A_{66S} constant (linear) and A_{66S} and A variable (present theory):

a) and b) wing box n.2 without, and with, a rib bolted at the centre of the beam, respectively.

c) and d) wing box n.3 without, and with, a rib bolted at the centre of the beam, respectively.

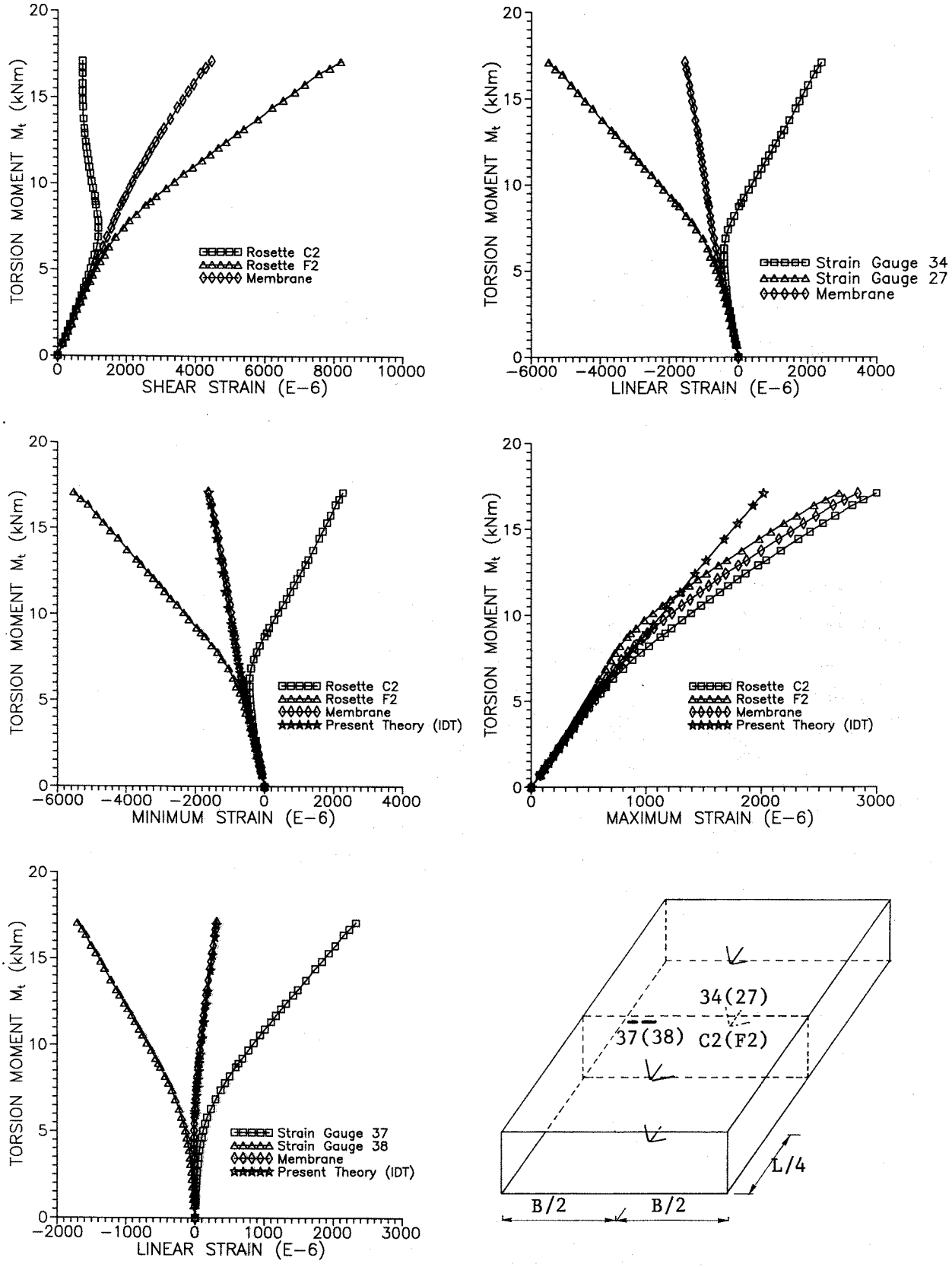

FIGURE 6 - Torsion moment versus experimental strains of wing box n.3, with a rib: a) Shear strain as obtained by back to back rosettes and by average values (membrane); b) linear strain at 45 deg; c) and d) Minimum and maximum strains along the two principal directions; e) Strains in the transverse direction.

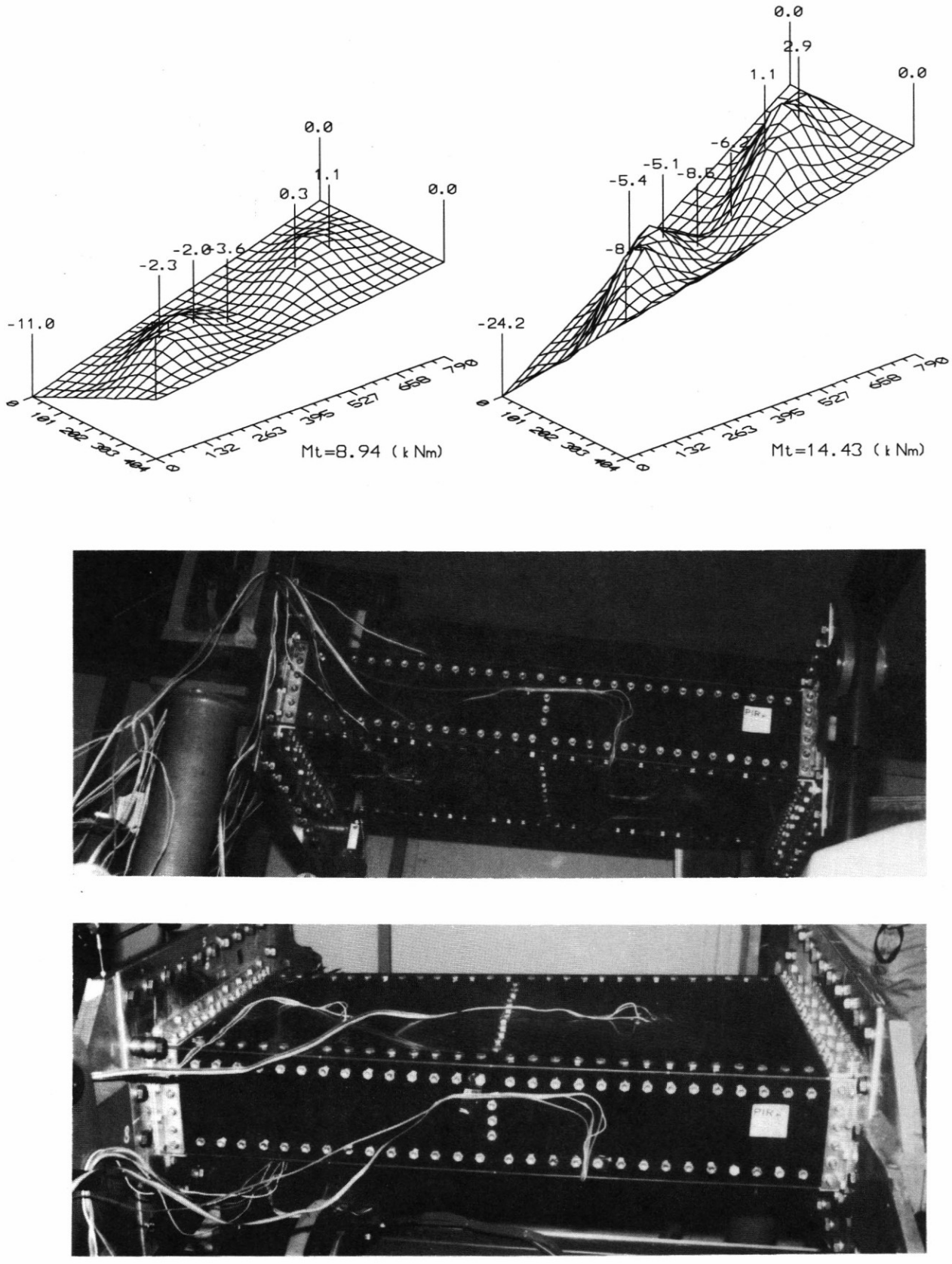

FIGURE 7 - Experimental out-of-plane deflection of wing box n.3, with a rib, at two values of applied twist moment. Skin panel failure.